RESEARCH ARTICLE



Ubiquitin specific peptidase 47 promotes proliferation of lung squamous cell carcinoma

Lin Yu^{1,2} · Jiayu Fu³ · Chunjian Shen³

Received: 2 November 2021 / Accepted: 10 February 2022 / Published online: 7 March 2022 © The Author(s) under exclusive licence to The Genetics Society of Korea 2022

Abstract

Background Ubiquitin specific peptidase 47 (USP47) is a kind of deubiquitinase, which has been reported to play oncogenic roles in several malignancies including colorectal cancer and breast cancer.

Objective Here we aimed to investigate the clinical significance of USP47 in lung squamous cell carcinoma (LUSC). **Methods** We retrospectively enrolled a cohort of LUSC patients who underwent surgical resection in our hospital (n=280)

Methods We retrospectively enrolled a cohort of LUSC patients who underwent surgical resection in our hospital (n=280) and conducted immunohistochemistry staining for their tumor tissues targeting USP47. The correlations between USP47 expression and clinicopathological characteristics were evaluated by Chi-square test. Univariate and multivariate analyses were conducted to assess the prognostic predictive role of USP47 in LUSC. Cell lines and mice models were utilized to explore the tumor-related functions of USP47 in vitro and in vivo, respectively.

Results Among the 280 cases, there were 127 cases classified as high-USP47 expression and 153 cases with low-USP47 expression. Statistical analyses revealed that higher USP47 expression was independently correlated with larger tumor size, advanced T stage, and unfavorable prognosis. Knockdown of USP47 by shRNA resulted in impaired proliferation of LUSC cell lines and reduced nucleus beta-catenin level. Furthermore, xenograft assays demonstrated that silencing USP47 can inhibit LUSC tumor growth in vivo.

Conclusion Our research established a novel tumor-promoting effect and prognostic predictive role of USP47 in LUSC, thereby providing evidence for further therapeutic development.

Keywords Lung squamous cell carcinoma · Proliferation · Prognosis · Ubiquitin specific peptidase 47 · Xenografts

Introduction

Lung cancer ranks the most frequent malignancy and the leading cause of tumor-associated deaths in the world (Siegel et al. 2016). More than 80% lung cancers can be pathologically defined as non-small cell lung cancer (NSCLC), which includes lung squamous cell carcinoma (LUSC) and lung adenocarcinoma. LUSC is usually originated from bronchi (Gridelli et al. 2015), which is characterized with unsatisfied prognosis (Diaz-Garcia et al. 2013). Identifying novel

biomarkers for prognostic prediction as well as therapeutic development is therefore critically needed (Tang et al. 2018; Wang et al. 2021; Yan et al. 2021; Yang et al. 2021).

Ubiquitin specific peptidase 47 (USP47) belongs to a family of ubiquitin-specific cysteine proteases, which functions by catalyzing the removal of ubiquitin from protein substrates that are ubiquitinated (Quesada et al. 2004). As an enzyme, the function of USP47 depends on its downstream substrates and plays vital roles in different cellular processes including carcinogenesis and cancer progression. For example, immunofluorescence staining data revealed that USP47 was upregulated in colorectal adenocarcinoma (CRC) tissues than that in nontumorous adjacent tissues (Choi et al. 2017), indicating its potential involvement in CRC. Indeed, later it was reported that upregulation of USP47 was correlated with carcinogenesis and unfavorable prognosis of CRC patients, which may functions by maintaining the cancer cell stemness (Zhang et al. 2021). Besides, USP47 was found to be significantly

- ☐ Chunjian Shen s139457@163.com
- Dalian Medical University, Dalian 116044, China
- Department of Thoracic Surgery, Dalian University Affiliated Xinhua Hospital, Dalian 116021, China
- Department of Cardiothoracic Surgery, Second Affiliated Hospital of Shenyang Medical College, 64 Qishan West Road, Shenyang 110035, China



upregulated in an epithelial-to-mesenchymal transition (EMT) model established using non-tumorigenic cell line MCF-10A cells, highlighting its participation in tumorigenesis (Silvestrini et al. 2020). Similarly, it has been suggested that USP47 may be required for HGF-induced wound healing of human pancreatic cancer cells (Buus et al. 2009). However, the expression pattern and function of USP47 in many other malignancies including lung cancers remain unknown.

In the current study, we initially investigated the protein expression level and clinical significance of USP47 in LUSC. In addition, the tumor-related role of USP47 was identified via knockdown strategy in two LUSC cell lines as well as in xenograft mice models.

Table 1 Correlations between USP47 expression and clinicopathological characteristics of LUSC patients

Patients and methods

Patients' information

We enrolled 280 primary LUSC cases (129 females and 151 males) who underwent surgical resection in our hospital with a median follow up time as 31 months (ranging 2–95 months). The patients' characteristics were summarized in Table 1. None of the patients underwent preoperative chemotherapy or other neoadjuvant therapies, but 88 cases (88/280, 31.4%) accepted postoperative adjuvant therapy treatment including chemotherapy, radiotherapy, or targeted therapy, etc. According to the age at diagnosis, 121 cases were equal to or younger than 65 years old, and 159 cases were older than 65 years old. Well grade of

Variables	Cases (n = 280)	USP47 expression		P value
		Low $(n = 153)$	High $(n = 127)$	
Age (years)				0.831
≤65	121	67	54	
>65	159	86	73	
Gender				0.906
Females	129	70	59	
Males	151	83	68	
Differentiation grade				0.295
Well	41	27	14	
Moderate	134	71	63	
Poor	105	55	50	
Tumor site				0.155
Upper lung	195	112	83	
Middle/lower lung	85	41	44	
Laterality				0.386
Left lung	120	62	58	
Right lung	160	91	69	
Tumor size				< 0.001
< 30 mm	167	110	57	
30-50 mm	75	32	43	
> 30 mm	38	11	27	
T stage				< 0.001
T1	142	107	35	
T2	97	36	61	
T3-T4	41	10	31	
LN metastasis				0.130
Negative	206	107	99	
Positive	74	46	28	
Adjuvant therapy				0.126
Rejected or unknown	192	99	93	
Accepted	88	54	34	

USP47 ubiquitin specific peptidase 47, *LUSC* lung squamous cell carcinoma, *LN* lymph node *Statistically significant by Chi-square test



pathological differentiation was observed in 41 cases, moderate differentiation in 134 patients, and poor differentiation in the other 105 patients. Up to 160 cases showed tumor location in right lung, while the other 120 cases with tumor location in the left lung. There were 167 cases with tumor size less than 30 mm in diameter, 75 cases with tumor size 30–50 mm, and only 38 cases with tumor size larger than 50 mm. Accordingly, 142 patients were staged as stage T1, 97 cases as stage T2, and the other 41 cases as stage T3–T4. As for the lymph node status, 206 patients showed no metastatic lymph node, while the other 74 cases showed positive lymph nodes.

GEPIA

Bioinformatic analysis was performed using Gene Expression Profiling Interactive Analysis (GEPIA) (http://gepia.cancer-pku.cn/#analysis) and the Human Protein Atlas (https://www.proteinatlas.org/) based on the data from The Cancer Genome Atlas (TCGA).

Immunohistochemistry (IHC)

IHC was conducted to explore the USP47 protein expression level in clinical tissue samples. Briefly, the tissue sections were deparaffinized, rehydrated, and then incubated with 3% hydrogen peroxide (H₂O₂). Antigen retrieval was achieved by using ethylene-diamine-tetra acetic acid (EDTA) buffer. The tissue sections were blocked with 5% bovine serum (BSA) and then probed with anti-USP47 antibody (1:300, Thermo Fisher Scientific) at 4 °C overnight. Secondary antibody was then added and incubated. The immunoreactivity was finally detected by using the diaminobenzidine (DAB) staining reagents according to the manufacturer's instructions (Liu et al. 2021). The IHC results were next scored regarding both staining intensity and the percentage of positively stained cells. Staining intensity was scored as negative staining: (-); weak staining: (+); moderate staining: (++); and strong staining: (+++). Accordingly, slides with more than 30% moderate stained cells (++) were regarded as high-USP47 expression; otherwise, the slides were grouped as low-USP47 expression.

Cell culture and shRNA infection

Human LUSC cell lines (SK-MES-1 and Calu-1) were acquired from the American Tissue Culture Collection (ATCC). All cells were routinely maintained in RPMI 1640 medium containing 10% fetal bovine serum (FBS). The cells were cultured in 37 °C incubator with 5% carbon dioxide.

The shRNAs targeting USP47 were constructed in pLVTHM lentiviral vectors (Sigma) with the following sequences. Scrambled shRNA: TTCTCCGAACGT

GTCACGT; shRNA#1: GAATCTGTCTTGAAACCA A; shRNA#2: GCAATGACTTGCTATTTGAA. Briefly, pLVTHM-shRNAs were co-transfected with the packaging vector psPAX2 and the envelope vector pMD2.G into HEK293T cells using LipofectamineTM 2000 reagent. The culturing media containing virus were harvested at 24 h post-transfection. LUSC cells were then infected with lentivirus medium mentioned above. After infection for three repeats, the knockdown efficiencies were determined by western blotting. The pLVTHM-scrambled shRNA was used as negative control.

Protein extraction and subcellular fractionation

Total protein in cultured cells was extracted using radio immunoprecipitation assay (RIPA) lysis buffer (P0013B, Beyotime) supplemented with protease and phosphatase inhibitors (P1051, Beyotime) along with 0.1 mM phenylmethylsulfonyl fluoride (PMSF) (ST506, Beyotime).

Cell fractionation and nuclear protein extraction were performed using the Nuclear and Cytoplasmic Protein Extraction Kit (P0028, Beyotime) according to the standard protocols. The BCA assay (Thermo Fisher Scientific) was used to detect protein concentration.

Western blot (WB) assay

Equal amount of protein samples was subjected to sodium dodecyl sulfate–polyacrylamide gel electrophoresis (SDS-PAGE) (P0012A, Beyotime), and then transferred to polyvinylidene fluoride (PVDF) membrane (IPSN07852, Millipore, Bedford, MA, USA). Next, membranes were incubated with primary antibodies at 1:1000 dilution at 4 °C overnight, then washed by 0.1 M TBST (TBS containing 0.1% Tween-20) for three times, followed by incubation with horseradish peroxidase-conjugated secondary antibodies for 1 h at room temperature. Finally, the immunoreactivities were tested using the ECL Western Blotting Substrate (Biotech, Beijing, China).

CCK-8 assays

Cell Counting Kit-8 assay (CCK-8, Donjindo, Tokyo, Japan) was introduced to evaluate the cell viability. Stably infected cells were seeded into 96-well plates and cultured for designated time points. Then $10~\mu L$ CCK8 reagents per well were added and the plates were incubated for additional 4 h. Then the absorbance at 450 nm was measured using a microplate reader to assess cell viability.



Colony formation

Single-cell suspensions of LUSC cells were seeded into 6-well plates at 1000 cells/well and incubated at 37 °C for 14 days. Then cells were fixed with 4% formaldehyde for 30 min, followed by staining with crystal violet solution for another 30 min. Then numbers of colonies were counted. Each experiment was repeated for three times.

Xenografts

The animal experiments were conducted with the approval by the Ethics Committee of our hospital. BALB/c nude mice were purchased from Shanghai Experimental Animal Center (China). shRNA-infected cells were collected and subcutaneously injected into nude mice. The growth of xenografts was monitored every week using a vernier caliper for four weeks. The tumor volume was counted via the equation: volume = $0.5 \times \text{length} \times \text{width} \times \text{width}$. After four weeks, all the mice were sacrificed for xenograft isolation (Chen et al. 2021).

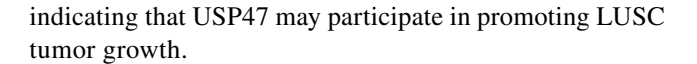
Statistical analysis

Cancer-specific survival (CSS) was defined as the period between surgical resection to the time of death caused by LUSC. All data were analyzed using SPSS20.0 and results were expressed as mean \pm SEM. The survival of LUSC patients was assessed using Kaplan–Meier survival analysis and compared by log-rank test. Differences between two groups were analyzed using the Student's t test and differences between three or more groups were analyzed using one-way analysis of variance (ANOVA) test. P < 0.05 was considered with statistical significance.

Results

Expression and clinical relevance of USP47 in LUSC

IHC data revealed a distinct protein expression pattern of USP47 in LUSC samples, therefore we grouped the cohort into high-USP47 group (n=127, Fig. 1a) and low-USP47 group (n=153, Fig. 1b). By evaluating the correlations between USP47 expression with clinicopathological characteristics using Chi-square test, we found that tumors with larger size were more prevalent to show higher USP47 protein staining intensity (P < 0.001, Table 1). Consistently, USP47 protein expression was also positively correlated with the tumor T stage (P < 0.001),



Prognostic analyses of LUSC cohort

Kaplan–Meier analyses were next conducted to further estimate the clinical significance of USP47 in LUSC. As shown in Fig. 1c, patients with higher USP47 expression showed a significant worser CSS than those with lower USP47 expression (P=0.019). The mean CSS time of high-USP47 group was 62.4 ± 3.9 months, while was 67.1 ± 2.8 months in low-USP47 group (Table 2). The 5-year CSS rate of high-USP47 group was 57.9%, while was 68.7% in low-USP47 group. Moreover, we extracted the data from TCGA datasets and found that a higher mRNA level of USP47 can also serve as an unfavorable prognostic factor for the disease-free survival (P=0.006, Fig. 1d) and overall survival (P=0.015, Fig. 1e) of LUSC patients.

Besides USP47 expression level, the prognostic effects of other enrolled factors were also analyzed (Fig. 2, Table 2). Accordingly, larger tumor size, advanced T stage, positive lymph nodes, and adjuvant chemotherapy were all identified as unfavorable prognostic factors based on univariate analyses (Table 2). However, the tumor size and adjuvant therapy lost their statistical significance in the further multivariate analysis (Table 3), indicating that they were not independent prognostic factors in our cohort. In contrast, T3–T4 tumor stage (HR = 2.613, 95% CI 1.050–4.457) and positive lymph nodes (HR = 2.217, 95% CI 1.252–3.928) were identified as independent prognostic factors. Of note, higher USP47 protein expression (HR = 1.911, 95% CI 1.136–3.213) was also confirmed as a novel independent risk factor for unfavorable prognosis of LUSC patients.

USP47 exerts tumor-promoting effects in LUSC

Considering the clinical significance of USP47 in LUSC, we were engaged to further investigate its detailed tumor-related functions. Using specific shRNAs to knockdown USP47 expression, we found that there was no significant alteration on the total beta-catenin level compared to the scrambled-shRNA-infected cells (Fig. 3a). However, the nucleus beta-catenin level was significantly downregulated after silencing USP47 in both the two LUSC cell lines, indicating that USP47 may exert tumor-promoting effects at least partially via modulating beta-catenin signaling. Indeed, CCK-8 assay (Fig. 3b) and colony formation data (Fig. 3c) revealed that USP47-shRNA can significantly inhibit the proliferation capacities of LUSC cell lines.

Finally, we conducted in vivo assays using xenograft mice model to validate the effects of USP47 in LUSC. According to the xenograft growth curves, the growth of USP47shRNA-infected xenografts was significantly slower than



Genes & Genomics (2022) 44:721-731

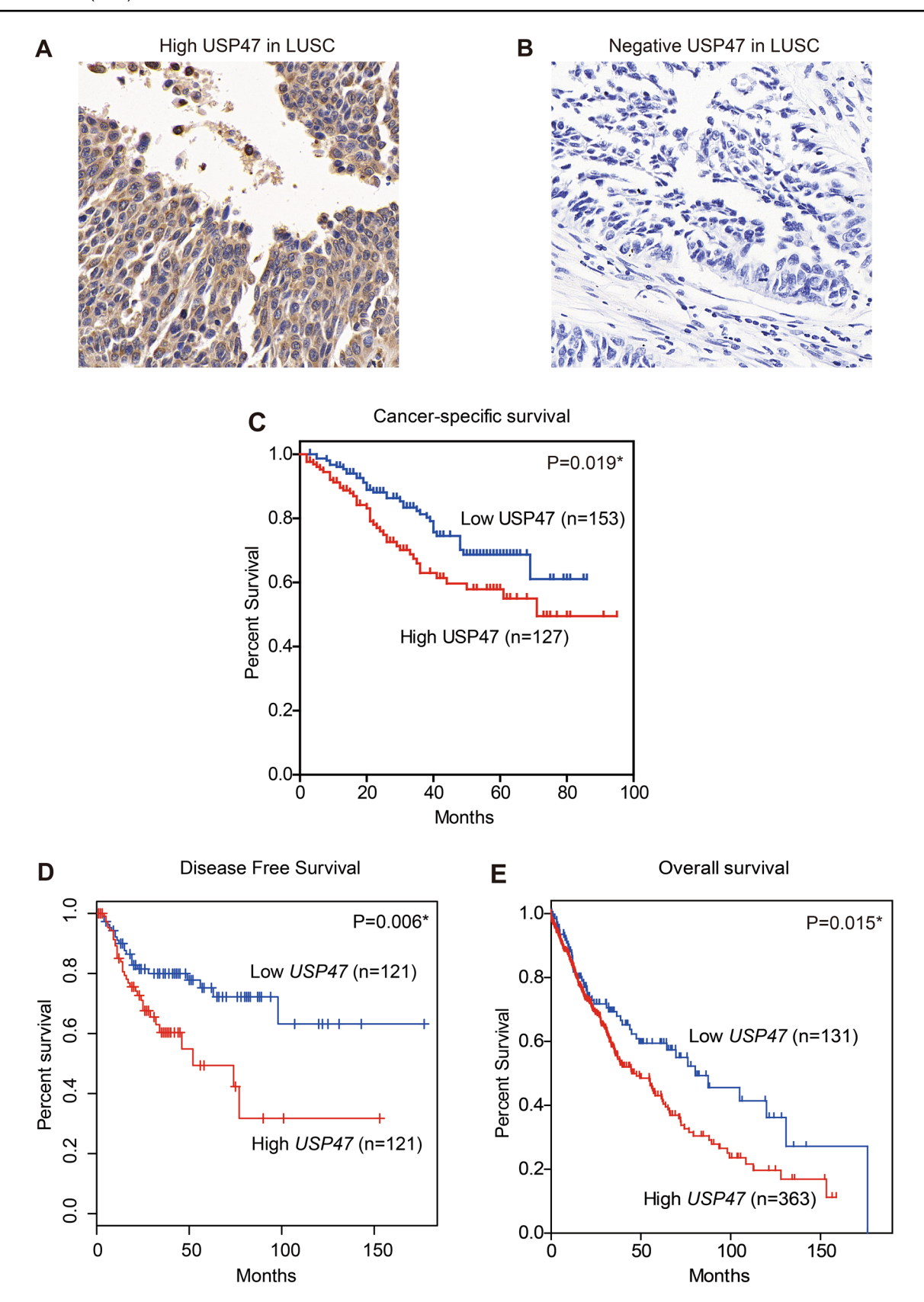


Fig. 1 Expression and predictive value of USP47 in LUSC. Immunohistochemistry staining showed representative high (a) and low (b) protein expression of USP47 in LUSC tissues. Kaplan–Meier curves

were plotted based on the protein levels of USP47 in our retrospective cohort (\mathbf{c}), or based on mRNA levels of USP47 in TCGA datasets (\mathbf{d} , \mathbf{e})



Table 2 Univariate analysis for the cancer-specific survival in LUSC patients

Variables	Cases $(n=105)$	Overall survival (months)		P value
		Mean ± SEM	5-year CSS (%)	
Age (years)				0.848
≤65	121	66.9 ± 3.8	60.3	
>65	159	63.0 ± 2.9	67.1	
Gender				0.467
Females	129	63.9 ± 3.0	66.3	
Males	151	66.5 ± 3.5	61.9	
Differentiation grade				0.167
Well	41	69.1 ± 4.4	78.0	
Moderate	134	66.1 ± 3.3	65.2	
Poor	105	62.8 ± 4.5	55.0	
Tumor site				0.945
Upper lung	195	68.7 ± 2.9	62.0	
Middle/lower lung	85	59.8 ± 3.6	68.9	
Laterality				0.456
Left lung	120	57.8 ± 3.3	65.8	
Right lung	160	69.5 ± 3.2	63.1	
Tumor size				0.007
< 30 mm	167	66.8 ± 2.7	71.1	
30-50 mm	75	64.8 ± 5.0	55.4	
> 30 mm	38	53.4 ± 6.3	46.0	
T stage				< 0.001
T1	142	69.4 ± 2.9	75.0	
T2	97	66.3 ± 4.4	60.6	
T3-T4	41	45.6 ± 5.9	35.1	
LN metastasis				< 0.001
Negative	206	71.6 ± 2.6	71.8	
Positive	74	50.9 ± 5.2	42.6	
Adjuvant therapy				< 0.001
Rejected or unknown	192	68.6 ± 2.5	74.1	
Accepted	88	55.3 ± 4.4	43.4	
USP47 level				0.019
Low	153	67.1 ± 2.8	68.7	
High	127	62.4 ± 3.9	57.9	

USP47 ubiquitin specific peptidase 47, LUSC lung squamous cell carcinoma, LN lymph node, CSS cancer-specific survival

that of scrambled-shRNA-infected ones (Fig. 4a). Consistently, isolated xenografts showed small tumor size as well as tumor weight in USP47-shRNA infected groups (Fig. 4b, c).

Discussions

In this study, we identified USP47 as a novel predictor for the survival of LUSC patients who underwent surgical resection. According to our cohort, LUSC patients with higher USP47 protein expression level in the tumor tissues exhibited significantly poorer prognosis than those with lower USP47 protein expression in tumor tissues. Although this was a single center retrospective cohort, we validated our findings by utilizing the TCGA datasets. As a result, TCGA data revealed that LUSC patients with high *USP47*-mRNA level exhibited unfavorable overall survival and disease-free survival than those with low *USP47*-mRNA expression in tumor tissues. Combined with the multivariate analysis, we safely came to the conclusion that USP47 can serve as a novel independent prognostic predictor for LUSC patients.

Besides its correlation with prognosis, we also found that the expression level of USP47 was positively correlated with tumor size and T stage of LUSC patients. Therefore, we



^{*}Statistically significant by log-rank test

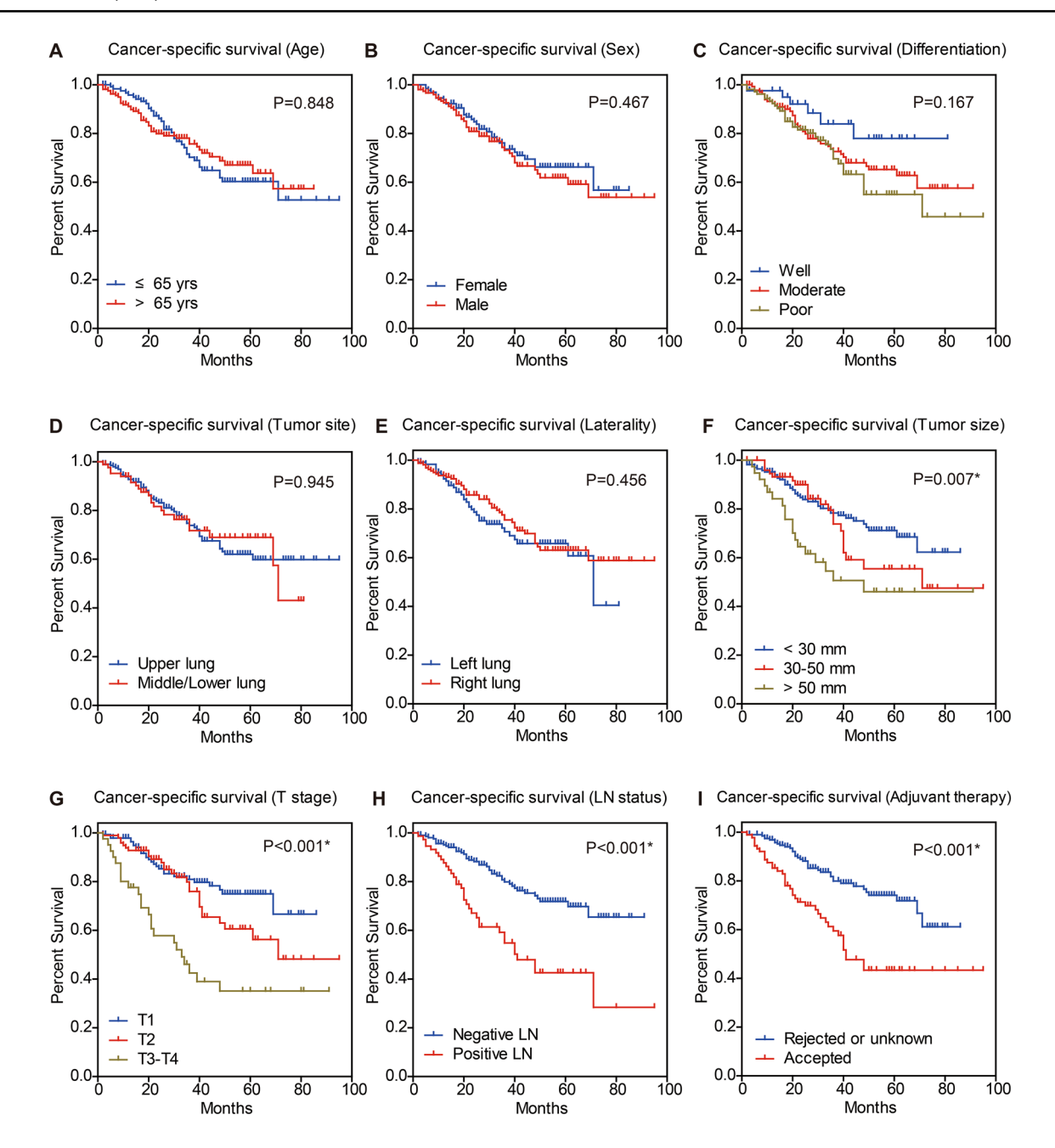


Fig. 2 Survival analyses of LUSC cohort. The prognostic value of all enrolled clinicopathological parameters were evaluated using Kaplan–Meier method and compared using log-rank test, including

patients' age (a), sex (b), differentiation grade (c), tumor site (d), tumor laterality (e), tumor size (f), T stage (g), lymph node metastasis (h), and adjuvant therapy (i)

conducted cellular assays by silencing USP47 in two LUSC cell lines, which demonstrated that USP47-knockdown would remarkably suppress lung cancer growth. The tumorinhibiting effect of USP47 was finally confirmed by using xenograft mice models, thus providing initial evidence on that targeting USP47 would be a potential direction for novel therapy development of LUSC.

Since this paper mainly focused on the clinical significance of USP47 in LUSC, we did not fully investigate its underlying signaling mechanisms. Nevertheless, immunoblotting data demonstrated that USP47-knockdown resulted in a significant decrease in the nucleus level of β -catenin without significant effect on the total β -catenin level in the whole cell lysate. Consistent with our findings, a previous report by Shi et al. showed that USP47 can directly deubiquitinate β -catenin, thus preventing its ubiquitination and degradation (Shi et al. 2015). Moreover, their data also found that USP47 shRNAs significantly decreased the protein level of nuclear



Table 3 Cox multivariate analysis for cancer-specific survival in LUSC patients

Variables	Hazard ratio	95% confidence interval	P value
Tumor size			
< 30 mm	Reference		
30-50 mm	0.848	0.456-1.577	0.602
> 30 mm	1.090	0.545-2.178	0.807
T stage			
T1	Reference		
T2	0.988	0.504-1.938	0.972
T3-T4	2.163	1.050-4.457	0.036*
LN metastasis			
Negative	Reference		
Positive	2.217	1.252-3.928	0.006*
Adjuvant therapy			
Rejected or unknown	Reference		
Accepted	1.608	0.884-2.927	0.120
USP47 level			
Low	Reference		
High	1.911	1.136-3.213	0.015*

USP47ubiquitin specific peptidase 47, LUSClung squamous cell carcinoma, LNlymph node

 β -catenin in HEK293T cells with or without Wnt treatment, which is also confirmed in our study in LUSC cells. Therefore, the crosstalk between USP47 and β -catenin signaling deserves further investigation.

Besides β -catenin, USP47 can also stabilize other protein substrates, subsequently exerts its tumor-related functions. For example, USP47 can regulate base excision repair by controlling steady-state level of DNA polymerase β . Knockdown of USP47 causes an increased ubiquitylation of Pol β , a decreased level of Pol β , and a subsequent deficiency in base excision repair, leading to accumulation of DNA strand breaks and consequently decreased cell viability in response to DNA damage (Parsons et al. 2011). Meanwhile, USP47 was found to counteract the ubiquitination of MAPKs induced by the N-end rule ligase POE/UBR4 in Drosophila, implying its involvement in MAPK signaling (Ashton-Beaucage et al. 2016). Although our data did not find a significant correlation between USP47 expression with LUSC metastasis, silencing of USP47 accelerated

the proteasomal degradation of Snail and inhibited EMT in colon cancers (Choi et al. 2017) as well as in MCF-10A cells (Silvestrini et al. 2020). Other reported substrates of USP47 in colon cancer cells include Stabilin 1 (Yu et al. 2019) and yes-associated protein 1 (Pan et al. 2020), both participate in modulating cell proliferation. In addition to the proliferation and invasion processes, USP47 also participates in modulating the cytotoxic effects of anticancer drugs via stabilizing Cdc25A (Peschiaroli et al. 2010) and β -transducin repeat-containing protein (β TrCP) (Naghavi et al. 2018).

USP47 can be regulated by various upstream regulators. For example, expression of USP47 can be directly inhibited by microRNAs (miR) including miR-204-5p in gastric cancer cells (Zhang et al. 2015), miR-199b (Guo et al. 2020) and miR-188-5p (Yan et al. 2019) in colon cancer cells, miR-101-3p in osteosarcomas (Zhang et al. 2020), miR-204-5p in ovarian cancer cells (Hu et al. 2019), and miR-454 in nasopharyngeal carcinoma cells (Yuan et al. 2021). Besides, endoplasmic reticulum aminopeptidase 1 (ERAP1) was reported to bind with USP47, thus displacing USP47-associated substrates such as βTrCP, which affected the Hedgehog-dependent tumorigenesis (Bufalieri et al. 2019).

As a functional enzyme with tumor-related roles, USP47 has been attracting more and more attentions on developing its specific inhibitors (Weinstock et al. 2012) including small-molecule allosteric inhibitors (Engström et al. 2020) and natural drugs (Zhang et al. 2021). Indeed, several USP47 inhibitors had been reported to possess antitumor potentials. For example, P5091 can inhibit expression of EMT markers and reverted morphological changes in MCF-10A cells that undergoing EMT (Silvestrini et al. 2020). Another example is that P22077 exerts cytotoxicity to chronic myeloid leukemia (CML) both in vitro and in vivo, which can also eliminate leukemia stem/progenitor cells in CML mice (Lei et al. 2021). Therefore, targeting USP47 would be an invaluable direction for novel therapeutic development in malignancies.

Conclusions

Taken together, USP47 is highly expressed in LUSC tissues and correlated with aggressive tumor characteristics as well as unfavorable prognosis, which may function through promoting tumor proliferation. Silencing USP47 can significantly impair LUSC progression, thus may serve as a novel therapeutic target and prognostic biomarker.



^{*}Statistically significant by Cox regression test

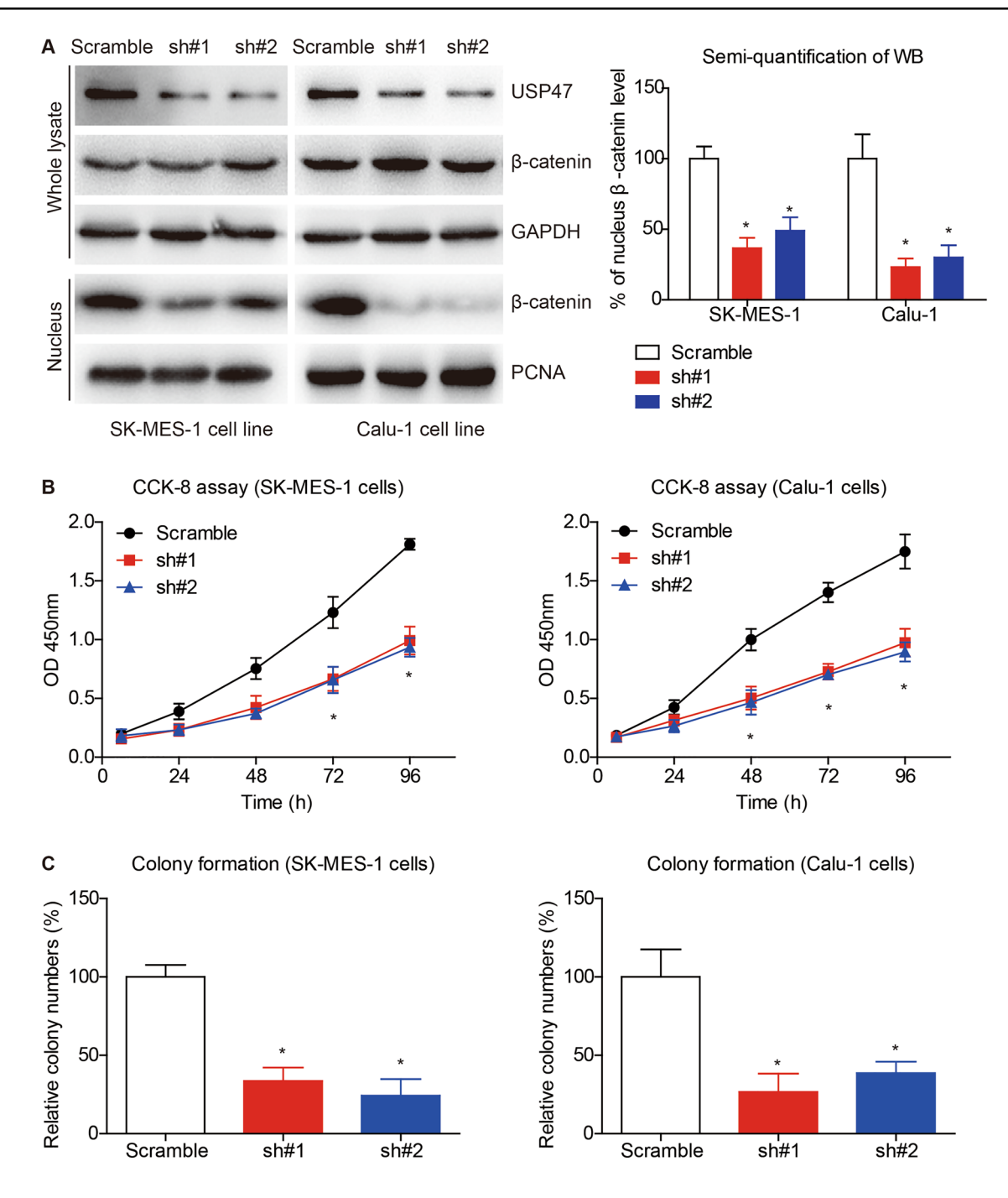
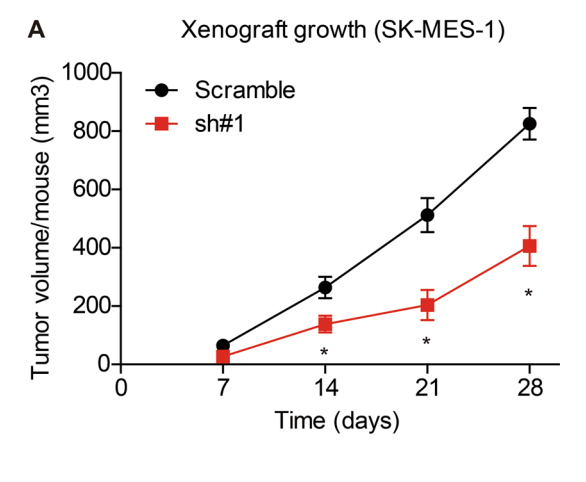
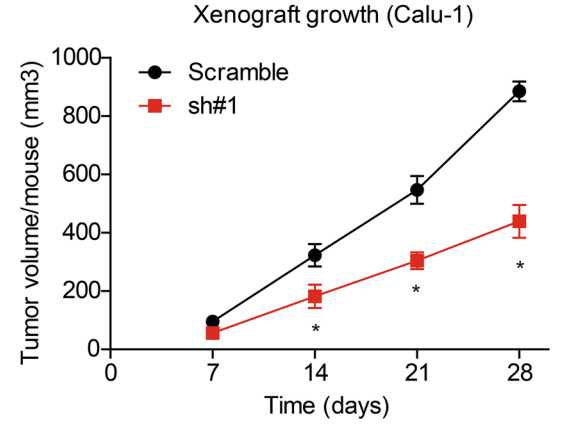


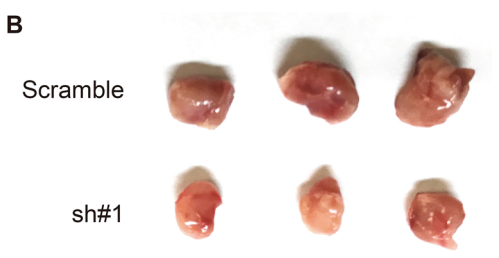
Fig. 3 Silencing USP47 decreases nucleus beta-catenin and inhibits LUSC growth. **a** Silencing USP47 by shRNAs resulted in significant decrease in nucleus beta-catenin level without affecting its entire expression in whole cell lysate. **b** CCK-8 assays revealed that USP47-

shRNAs can attenuate LUSC cell viability. c Comparing with control groups infected with scramble shRNA, USP47-shRNA infected cells showed an impaired capacity in colony formation. *P<0.05 by one-way ANOVA test





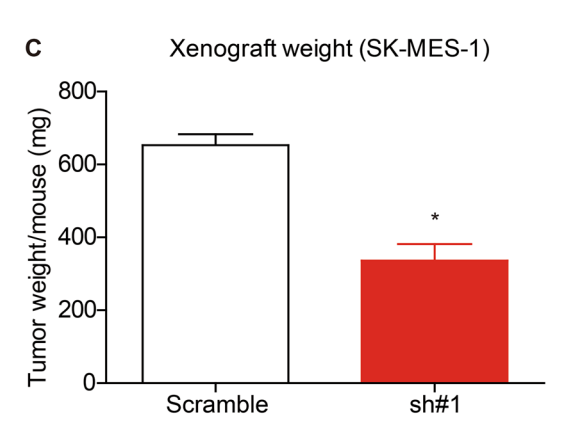




sh#1

Scramble

Xenografts generated by SK-MES-1 cells



Xenografts generated by Calu-1 cells

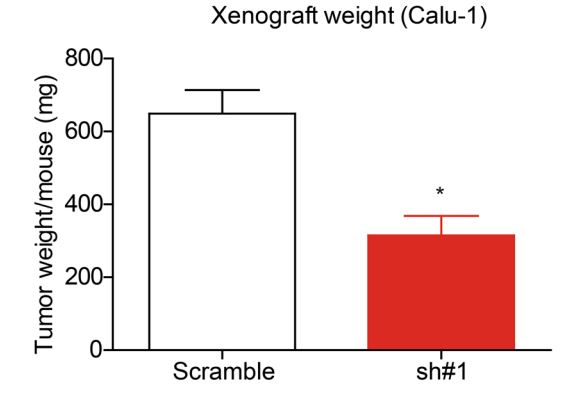


Fig. 4 Silencing USP47 inhibits LUSC growth in vivo. **a** The growth of subcutaneous implanted xenografts was monitored and plotted. **b** The excised tumors were photographed, which showed a significant

smaller tumor size in USP47-shRNA group. $\bf c$ The isolated xenografts were weighted, showing a consistent lower weight in USP47-shRNA groups than control ones. *P<0.05 by Student's t-test

Funding None.

Declarations

Conflict of interest Author Lin Yu, author Jiayu Fu, and author Chunjian Shen declare that they have no conflict of interest.

Ethics This study was conducted in accordance with the Declaration of Helsinki and approved by the Ethics Committee of Dalian Medical University. Written informed consents were obtained from all partici-

pants. The animal study was approved and supervised by the Animal Center of Dalian Medical University.

Data availability Data will be available upon reasonable request.

References

Ashton-Beaucage D, Lemieux C, Udell CM, Sahmi M, Rochette S, Therrien M (2016) The deubiquitinase USP47 stabilizes MAPK



- by counteracting the function of the N-end rule ligase POE/UBR4 in Drosophila. PLoS Biol 14:e1002539
- Bufalieri F, Infante P, Bernardi F, Caimano M, Romania P, Moretti M, Severini LL, Talbot J, Melaiu O, Tanori M (2019) ERAP1 promotes Hedgehog-dependent tumorigenesis by controlling USP47-mediated degradation of βTrCP. Nat Commun 10:1–15
- Buus R, Faronato M, Hammond DE, Urbé S, Clague MJ (2009) Deubiquitinase activities required for hepatocyte growth factorinduced scattering of epithelial cells. Curr Biol 19:1463–1466
- Chen T, Liu H, Liu Z, Li K, Qin R, Wang Y, Liu J, Li Z, Gao Q, Pan C (2021) FGF19 and FGFR4 promotes the progression of gallbladder carcinoma in an autocrine pathway dependent on GPBAR1-cAMP-EGR1 axis. Oncogene 30:4941–4953
- Choi B-J, Park S-A, Lee S-Y, Cha YN, Surh Y-J (2017) Hypoxia induces epithelial—mesenchymal transition in colorectal cancer cells through ubiquitin-specific protease 47-mediated stabilization of Snail: a potential role of Sox9. Sci Rep 7:1–15
- Diaz-Garcia CV, Agudo-Lopez A, Perez C, Lopez-Martin JA, Rodriguez-Peralto JL, de Castro J, Cortijo A, Martinez-Villanueva M, Iglesias L, Garcia-Carbonero R et al (2013) DICER1, DROSHA and miRNAs in patients with non-small cell lung cancer: implications for outcomes and histologic classification. Carcinogenesis 34:1031–1038
- Engström O, Belda O, Kullman-Magnusson M, Rapp M, Böhm K, Paul R, Henderson I, Derbyshire D, Karlström S, Parkes KE (2020) Discovery of USP7 small-molecule allosteric inhibitors. Bioorg Med Chem Lett 30:127471
- Gridelli C, Rossi A, Carbone DP, Guarize J, Karachaliou N, Mok T, Petrella F, Spaggiari L, Rosell R (2015) Non-small-cell lung cancer. Nat Rev Dis Primers 1:15009
- Guo X, Liu L, Zhang Q, Yang W, Zhang Y (2020) E2F7 transcriptionally inhibits microRNA-199b expression to promote USP47, thereby enhancing colon cancer tumor stem cell activity and promoting the occurrence of colon cancer. Front Oncol 10:565449
- Hu L, Kolibaba H, Zhang S, Cao M, Niu H, Mei H, Hao Y, Xu Y, Yin Q (2019) MicroRNA-204-5p inhibits ovarian cancer cell proliferation by down-regulating USP47. Cell Transplant 28:51S-58S
- Lei H, Xu H-Z, Shan H-Z, Liu M, Lu Y, Fang Z-X, Jin J, Jing B, Xiao X-H, Gao S-M (2021) Targeting USP47 overcomes tyrosine kinase inhibitor resistance and eradicates leukemia stem/progenitor cells in chronic myelogenous leukemia. Nat Commun 12:1–16
- Liu H, Gong Z, Li K, Zhang Q, Xu Z, Xu Y (2021) SRPK1/2 and PP1 α exert opposite functions by modulating SRSF1-guided MKNK2 alternative splicing in colon adenocarcinoma. J Exp Clin Cancer Res 40:1–16
- Naghavi L, Schwalbe M, Ghanem A, Naumann M (2018) Deubiquitinylase USP47 promotes RelA phosphorylation and survival in gastric cancer cells. Biomedicines 6:62
- Pan B, Yang Y, Li J, Wang Y, Fang C, Yu F-X, Xu Y (2020) USP47mediated deubiquitination and stabilization of YAP contributes to the progression of colorectal cancer. Protein Cell 11:138–143
- Parsons JL, Dianova II, Khoronenkova SV, Edelmann MJ, Kessler BM, Dianov GL (2011) USP47 is a deubiquitylating enzyme that regulates base excision repair by controlling steady-state levels of DNA polymerase β. Mol Cell 41:609–615
- Peschiaroli A, Skaar J, Pagano M, Melino G (2010) The ubiquitinspecific protease USP47 is a novel β-TRCP interactor regulating cell survival. Oncogene 29:1384–1393
- Quesada V, Diaz-Perales A, Gutiérrez-Fernández A, Garabaya C, Cal S, López-Otin C (2004) Cloning and enzymatic analysis of 22

- novel human ubiquitin-specific proteases. Biochem Biophys Res Commun 314:54–62
- Shi J, Liu Y, Xu X, Zhang W, Yu T, Jia J, Liu C (2015) Deubiquitinase USP47/UBP64E regulates β -catenin ubiquitination and degradation and plays a positive role in Wnt signaling. Mol Cell Biol 35:3301–3311
- Siegel RL, Miller KD, Jemal A (2016) Cancer statistics, 2016. CA Cancer J Clin 66:7–30
- Silvestrini VC, Thomé CH, Albuquerque D, de Souza Palma C, Ferreira GA, Lanfredi GP, Masson AP, Delsin LEA, Ferreira FU, de Souza FC (2020) Proteomics analysis reveals the role of ubiquitin specific protease (USP47) in epithelial to mesenchymal transition (EMT) induced by TGFβ2 in breast cells. J Proteom 219:103734
- Tang W, Wan S, Yang Z, Teschendorff AE, Zou Q (2018) Tumor origin detection with tissue-specific miRNA and DNA methylation markers. Bioinformatics 34:398–406
- Wang Z, Xiang H, Dong P, Zhang T, Lu C, Jin T, Chai KY (2021) Pegylated azelaic acid: synthesis, tyrosinase inhibitory activity, antibacterial activity and cytotoxic studies. J Mol Struct 1224:129234
- Weinstock J, Wu J, Cao P, Kingsbury WD, McDermott JL, Kodrasov MP, McKelvey DM, Suresh Kumar K, Goldenberg SJ, Mattern MR (2012) Selective dual inhibitors of the cancer-related deubiquitylating proteases USP7 and USP47. ACS Med Chem Lett 3:789–792
- Yan S, Yue Y, Wang J, Li W, Sun M, Gu C, Zeng L (2019) LINC00668 promotes tumorigenesis and progression through sponging miR-188–5p and regulating USP47 in colorectal cancer. Eur J Pharmacol 858:172464
- Yan S, Yan J, Liu D, Li X, Kang Q, You W, Zhang J, Wang L, Tian Z, Lu W (2021) A nano-predator of pathological MDMX construct by clearable supramolecular gold (I)-thiol-peptide complexes achieves safe and potent anti-tumor activity. Theranostics 11:6833
- Yang Z, Lian Z, Liu G, Deng M, Sun B, Guo Y, Liu D, Li Y (2021) Identification of genetic markers associated with milk production traits in Chinese Holstein cattle based on post genome-wide association studies. Anim Biotechnol 32:67–76
- Yu L, Dong L, Wang Y, Liu L, Long H, Li H, Li J, Yang X, Liu Z, Duan G (2019) Reversible regulation of SATB1 ubiquitination by USP47 and SMURF2 mediates colon cancer cell proliferation and tumor progression. Cancer Lett 448:40–51
- Yuan F, Lou Z, Zhou Z, Yan X (2021) Long non-coding RNA KCN-Q1OT1 promotes nasopharyngeal carcinoma cell cisplatin resistance via the miR-454/USP47 axis. Int J Mol Med 47:1–1
- Zhang B, Yin Y, Hu Y, Zhang J, Bian Z, Song M, Hua D, Huang Z (2015) MicroRNA-204-5p inhibits gastric cancer cell proliferation by downregulating USP47 and RAB22A. Med Oncol 32:331
- Zhang S, Ding L, Gao F, Fan H (2020) Long non-coding RNA DSCAM-AS1 upregulates USP47 expression through sponging miR-101-3p to accelerate osteosarcoma progression. Biochem Cell Biol 98:600–611
- Zhang S, Ju X, Yang Q, Zhu Y, Fan D, Su G, Kong L, Li Y (2021) USP47 maintains the stemness of colorectal cancer cells and is inhibited by parthenolide. Biochem Biophys Res Commun 562:21–28

Publisher's Note Springer Nature remains neutral with regard to jurisdictional claims in published maps and institutional affiliations.

